

## The Generation of Calandria Tube (CT) Inner Diameter Profiles from Fuel Channel (FC) Inspection Data

**P.J.Sedran<sup>1</sup>, B. Rankin<sup>2</sup>, and C. Lemire<sup>3</sup>**

<sup>1</sup>Fuel Channels Consultant, AMEC NSS  
(paul.sedran@amec.com)

<sup>2</sup>NB Power  
(brankin@nbpower.com)

<sup>3</sup>Hydro-Québec  
(Lemire.Christian@hydro.qc.ca)

### **Abstract**

Studies of CT deformation at spacer locations, key to the development of FC deformation modelling, have been limited by the availability of gauging measurements from removed CTs. In [1], it was proposed that CT dimensional profiles could be generated using FC inspection data. Since then, the concept was investigated further by assessing: (1) the normalisation of gap measurements to the diameter of the spacer coil, (2) the validity of gap measurements from inspections of Point Lepreau and Gentilly-2, and the CT dimensional profiles generated from the inspection data. It was concluded, from the work presented in this paper, that the CT-PT gap data and the CT dimensional profiles generated using the data from the two subject inspections are reasonable.

### **1. Introduction**

The modelling of CT local creep deformation at spacer locations has been an active topic since 2001, when the first CT local ovality model was coded into CDEPTH 8.2. With the recent gauging of a small number of removed CTs, researchers have identified a need for additional CT inner diameter (ID) measurements [2] to be used to calibrate the modelling of local CT creep deformation at the spacers. Independent of that work, the generation of CT ID profiles from FC inspection data was demonstrated in [1], but, the proposed methodology was not implemented because the accuracy of the CT-PT gap data used at the time was challenged. Since that time, the following work has been performed to further research the use of FC inspection data to generate CT ID profiles:

1. An examination of CT-PT gap measurements from 2004 and 2005 from Point Lepreau, (PLGS) and Gentilly-2, (G-2)
2. An assessment of normalising the CT-PT gap measurements to the diameter of the spacer coil
3. The generation and assessment of CT ID profiles for PLGS and G-2.

### **2. Fuel Channel Inspection Data**

Details of the FC inspection data examined for this paper are presented in Table 1.

The inspection data used here are the PT ID, PT wall thickness, and CT-PT gap. Gap measurements are discussed in some detail but the others are not addressed, since the PT measurements have been standardised and are now routine, whereas the gap measurements are more recent developments.

**Table 1 – Details of CT-PT Gap Inspections**

FC	Inspection		FCs Inspected	Inspection Equipment	Measurement Spacing		Calibration	Gap Fitting Routine
	Date	EFPH			Axial (mm)	Angular (°)		
PLF06	May 2004	156,511	12	AFCIS	220	4.6	Gap at Spacer	Point Fit
G2H14	May 2005	161,000	15	SyDef Module	249.2	5	None	Point Fit & Circle Fit

Note: AFCIS is the AECL Advanced Fuel Channel Inspection System and SyDef is the inspection module developed by Hydro-Quebec for the SLAR Tool.

From Table 1, for the PLGS inspections, only point fit gap data were provided. For the G-2 inspections, both point and circle fit gap measurements were provided.

### 2.1 Processing of CT-PT Gap Measurement Data

The gap measurements obtained during FC inspections are subject to (1) circle and point fitting, and (2) calibration to the spacer coil outer diameter, covered in Sections 2.1.1 and 2.1.2.

#### 2.1.1 Circle and Point Fitting of Gap Data

CT-PT gap measurements are based on the detection of eddy current signal variations with gap, as the gap probe scans the FC. To measure the gap, the gap probe response requires calibration to known gap values. The calibration of the PLGS and G-2 gap measurements was based on a two stage process: (1) circle-fit routine- the gap around the circumference of the PT, to be correlated to the gap probe signal, was determined assuming that the PT and CT were circular. The gap measurements were then correlated to the known CT-PT gap, calculated from the measured PT dimensions and the CT as installed ID. The use of as-installed CT dimensions ignores CT deformation, but the average gap is not affected significantly. The gap measurement to the known gap correlation was used to derive a relationship between the gap measurement and the known gap. (2) point-fit routine - the above gap measurement to gap relationship is used directly to obtain the gap, not assuming circular geometries, allowing for more accurate gap measurements that capture the local deformation of the CT.

#### 2.1.2 Calibration of CT-PT Gap Measurements Based on the Spacer Coil Outer Diameter

In many channels, the measured gaps at the spacers were smaller than the nominal outer diameter of the spacer coil, (5.588 mm), and were thought to need correction. The calibration depicted in Figure 1 was typically used to adjust the measurements. The figure shows gap measurements at the bottom of the CT versus axial position along the length of the CT for G2H14. The lower blue line and the upper red line represent the measured and calibrated gaps. The grey triangles, plotted at a gap value of 5.588 mm, represent the spacers. Figure 2, which presents the calibrated gap versus the measured gap, details the numerical scheme that was used in the gap calibrations. The implications of this gap calibration are discussed later.

### 3. Examination of Historical CT-PT Gap Data from CANDU 6 Inspections

Figure 3 depicts the theoretical distribution of CT-PT gap vs angular position ( $\theta$ ) around the PT circumference, assuming perfectly circular tubes with nominal dimensions. Throughout this paper, the origin for angular position is at the top dead centre of the PT. The horizontal red line in Figure 3 represents the gap for a concentric PT and CT.

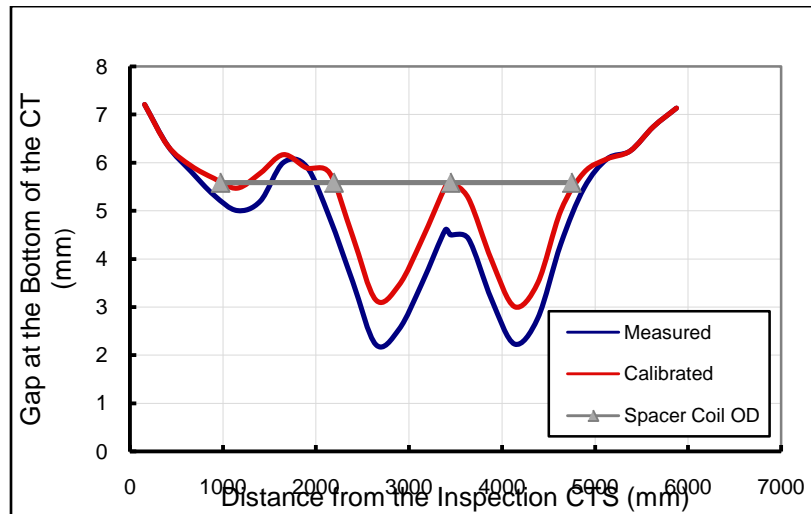


**Figure 1. Measured and Calibrated Gap at the Bottom of FC G2H14**

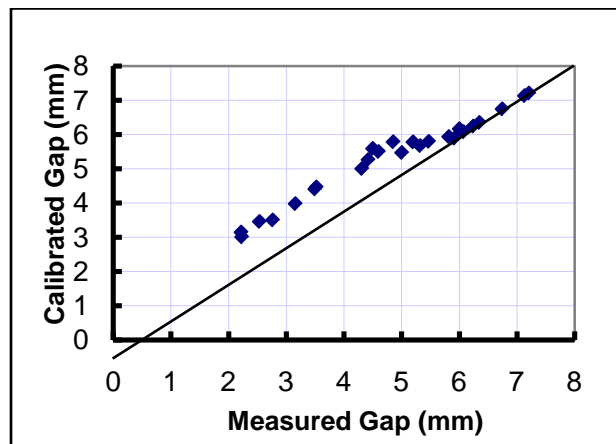


**Figure 2. Calibration Scheme for the Gap Measurements from the Inspection of G2H14**

The blue sinusoidal curve represents the gap at a spacer location, assuming no CT deformation at the point of contact with the spacer. Figure 3 is useful as a general guide for roughly judging the validity of gap measurements at a given axial location in the fuel channel.

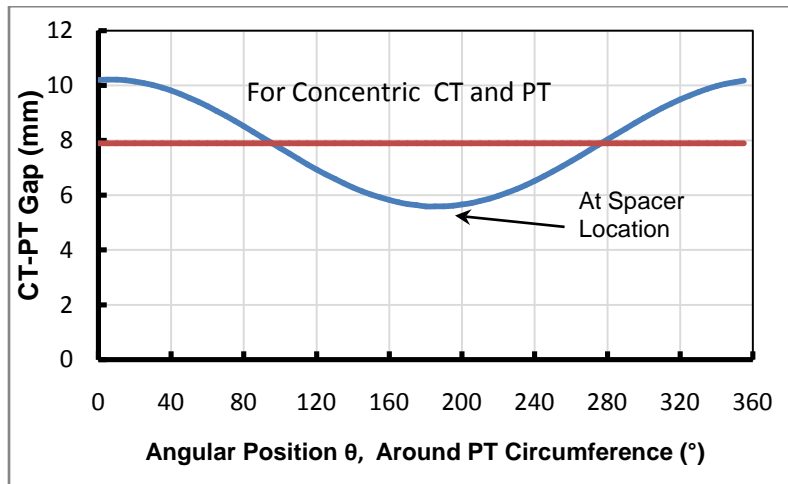


**Figure 3. Idealized CT-PT Circumferential Gap Distribution**

### 3.1 Gap Distribution Near the End of the PT

A verification of gap measurements was attempted by examining the circumferential gap distribution near the end of the PT, where CT and PT cross-sections are expected to be close to circular, presented in Figures 4 and 5, for PLF06 and G2H14, respectively. The gap profile of Figure 4 is located 139 mm inboard of the West Calandria Tube Sheet (CTS) and 268 mm inboard of the West end fitting taper. The measured gap is depicted as the blue line and the red line represents the expected gap, which was calculated based on PT sag measurements, assuming the following:

1. The PT and CT cross-sections remain circular and have design dimensions
2. During the gap measurement, the centreline of the deformed PT remained in a vertical plane

The PT sag at the axial location of the gap measurements of Figure 4 was found to be 1.42 mm. The measured gap in Figure 4 is in reasonable agreement with the expected gap, but is larger in the region from 280 to 80 degrees, at the top of the CT. The gap data in Figure 4 were calibrated by adjusting the gap to the spacer coil outer diameter. Since the gap calibration tends to increase the gap measurements, an explanation for Figure 4 is that the calibration resulted in an overestimation of the actual gap.

Figure 5 presents 3 gap distributions for G2H14 at 189.4 mm inboard of the North Calandria Tube Sheet (CTS) and 164.4 mm inboard of the North end fitting taper. The red undulating line is the point-fit gap and the blue line is the circle fit gap.

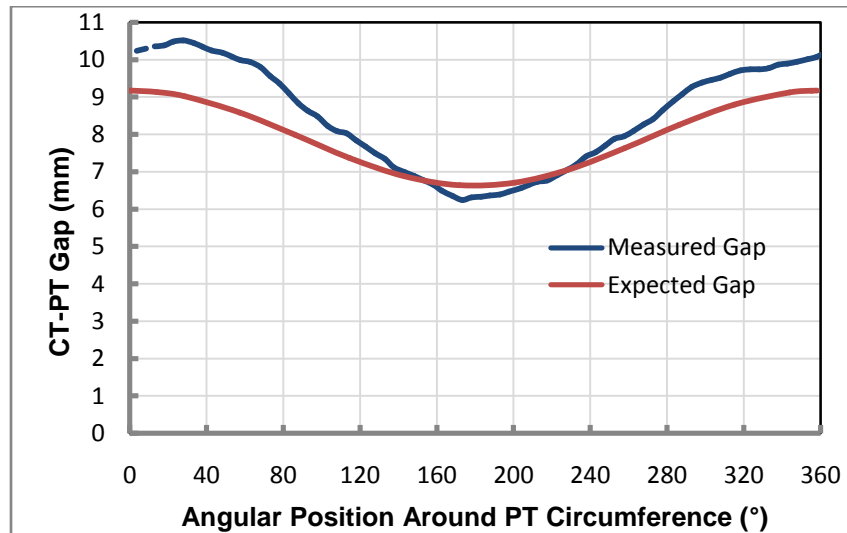


**Figure 4. Circumferential Gap Distribution for PLF06 139 mm Inboard of the West CTS**

The black curve represents the calculated gap for a measured PT sag of 4.94 mm at 189.4 mm inboard of the North CTS, for the same assumptions used for PLF06. The overall match of the circle-fit and point-fit gaps to the expected gap is reasonable. At various  $\theta$  values, the point-fit gap is closer to the expected gap than the circle-fit gap, indicating that the former is the better fit to the actual gap. However, the 1 mm undulations observed in the point-fit gap are not explicable by PT ID and wall thickness variations (0.2 mm). Regardless, Figures 4 and 5 indicate that the point-fit routine with no calibration of gap measurements produces the most accurate gap distribution near the ends of the CT.

### 3.2 Gap Distribution Between Spacers

The circumferential CT-PT gap distribution at the minimum gap location in G2H14, critical for CT-PT contact, is presented in Figure 6. The blue and red lines represent circle and point fits to the gap measurements, respectively. At the minimum gap location, the circle-fit and point-fit gaps are in close agreement, so either can be used to determine the minimum gap values. However, point-fitting provides a more detailed distribution for the gap around the circumference of the PT.

Considering Figures 4 – 6, it is recommended that the un-calibrated point-fit method be used to establish CT-PT gap distributions. However, point-fitting versus circle-fitting will not influence the minimum gap values at the bottom of the CT.

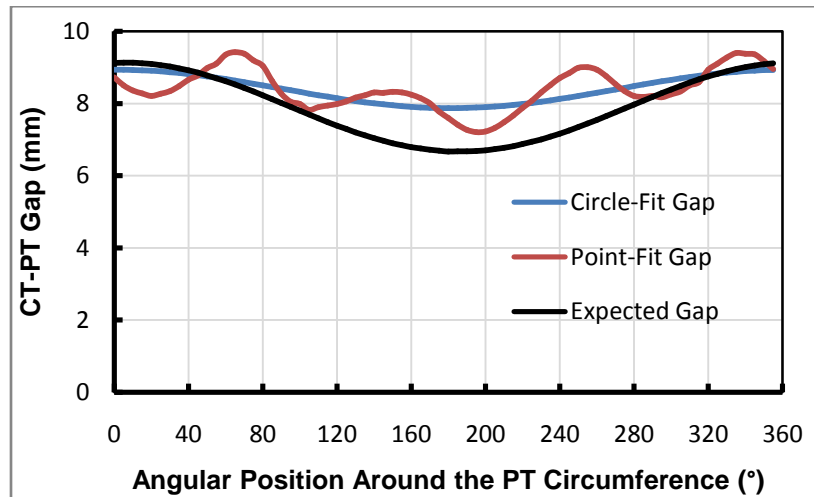


**Figure 5. Circumferential Distribution of the Gap in G2H14 189 mm Inboard of the North CTS**

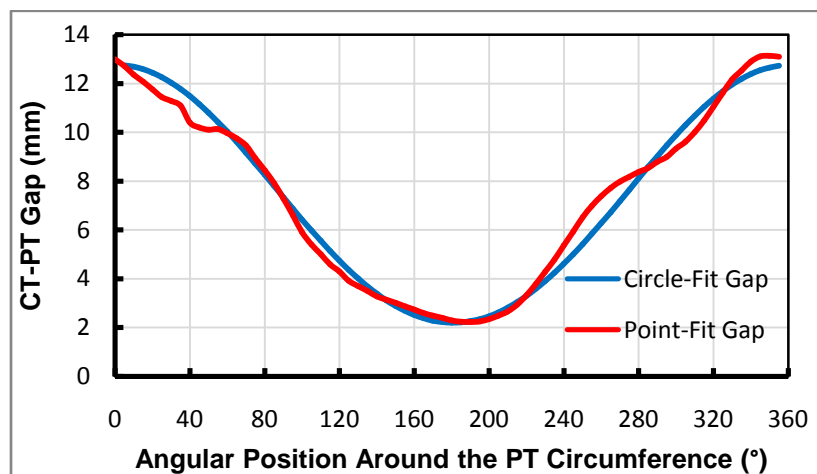


**Figure 6. Circumferential Gap Distribution in G2H14 at the Location of the Minimum Gap**

### 3.3 Gap Distribution at Spacer Locations

Figure 7 presents plots of the calibrated gap versus  $\theta$  at three spacer locations for PLF06. At the spacers, there are conspicuous unexplained irregularities in the gap distribution from 80 to 300°, the sector over which the spacer would be in contact with the CT.

### 3.4 Axial Distribution of CT-PT Gap

For this assessment, the gap measurements at 180° (at the bottom of the CT) were combined with PT sag and wall thickness measurements to generate a series of elevation points for the CT inner surface along the length of the CT. Here, elevation is defined as the vertical distance of a point below the reference plane, which is a horizontal plane tangent to the inside surface at the bottom of the PT, for a straight and horizontal PT.

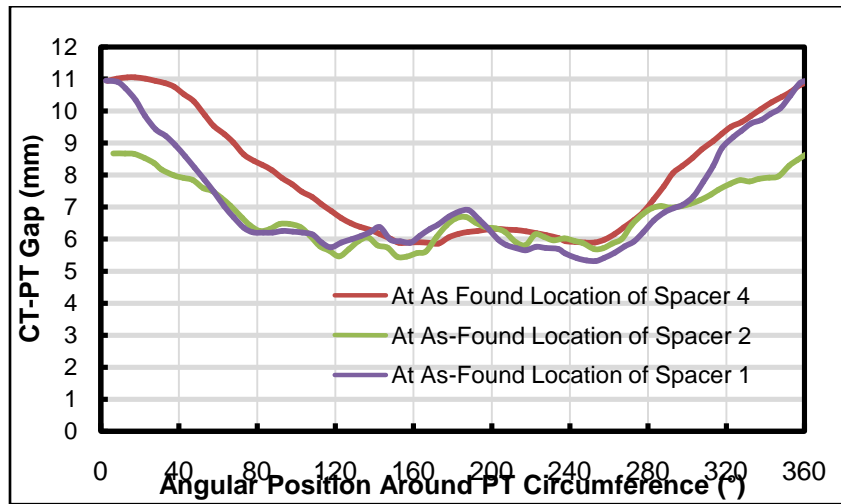


**Figure 7. Circumferential Gap Distribution in PLF06 at Spacer Locations**

The elevation of the CT bottom inner surface was determined using:

$$Y_{CT} = Y_{PT} - w_{PT} - \text{Gap}_{CT-PT}$$

Where  $Y_{CT}$  and  $Y_{PT}$  are the elevations of the CT and PT bottom inner surfaces;  $w$  is the wall thickness.

The resultant CT elevation profile and the elevations of the PT inner and outer surfaces for PLF06 are given in Figure 8.

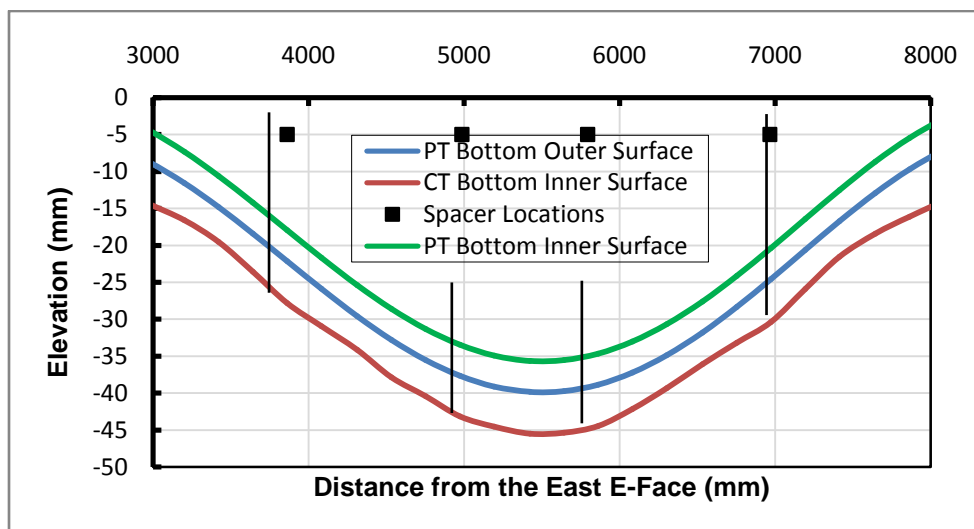


**Figure 8. Elevation Profiles for the Inner and Outer Surfaces of the PT and CT in PLF06**

The curves in the figure represent the intersection of the PT inner and outer surfaces and the CT inner surface with a vertical plane. The black square points in the figure indicate as-found spacer locations from the 1995 SLAR campaign. The elevation of the PT inner surface curve, depicted as the green line, was determined from the PT sag profile for PLF06, from the 2004 inspection. Although a quantitative evaluation of the results in Figure 8 is not possible, the following qualitative evaluation can be made. The

CT bottom inner surface elevation and that of the PT appear to be of similar form, as expected. In Figure 8, there are shallow depressions in the CT bottom inside surface at spacer locations 1, 2, and 4. The locations and extents of these depressions are consistent with those observed in removed CTs [2]. Although the assessment is not quantitative, there are no indications any of problems with the results in Figure 8.

#### 4. Generation of CT Inner Diameter ( ID) Profiles

Originally, FC inspections were limited to PT gauging and sag measurements, but, the addition of a gap probe module allowed for the determination of the radial distance from the centre of the PT to the inside surface of the CT ( $R_{CT}(\theta, x)$ ) at various angles ( $\theta$ ), where  $x$  is the axial position along the CT.  $R_{CT}(\theta, x)$  is the sum of PT inner radius plus the wall thickness and the PT-CT gap:

$$R_{CT}(\theta, x) = IR_{PT}(\theta, x) + w_{PT}(\theta, x) + gap(\theta, x) \quad (1)$$

where  $IR_{PT}$  and  $w_{PT}$  are the PT inner radius and wall thickness. For given values of  $x$  and  $\theta$ , the CT inner diameter is the sum of  $R_{CT}(\theta, x)$  and the radial distance diametrically opposite to it:

$$ID_{CT}(\theta, x) = R_{CT}(\theta, x) + R_{CT}(\theta + 180^\circ, x) \quad (2)$$

Using Equations (1) and (2), CT ID values at angular orientations ranging from 0 to 180° were generated for various cross-sections along the length of the CT for PLF06 and G2H14. The CT ID values were used to produce axial distributions of minimum, average, and maximum CT ID, and circumferential profiles of CT ID at spacer locations, presented in Sections 4.1 and 4.2.

##### 4.1 CT ID Profiles for PLF06

Figure 9 presents axial CT ID profiles (maximum, mean and minimum ID values along the length of the CT) for PLF06, using calibrated gap measurements. Also plotted in the figure are the four as-found spacer locations from the 1995 inspection of the channel, which were close to the as-found locations in the 2004 inspection. The circumferential CT ID profile for the CT, at 4700 mm from the East CTS, close to spacer 4, is presented in Figure 10.

##### 4.2 CT ID Profiles for G2H14

Figure 11 presents axial CT ID profiles for G2H14, using uncalibrated gap measurements, along with the four as-found spacer locations from the 2005 inspection. A circumferential CT ID profile for the CT cross-section located at 1930 mm from the North CTS, close to Spacer 2, is presented in Figure 12.

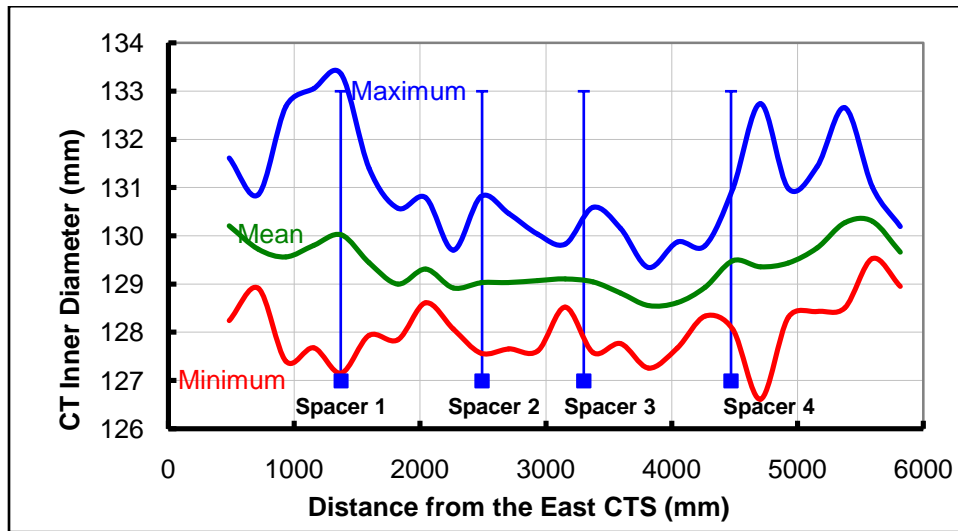


Figure 9. Axial CT ID Profiles for PLF06

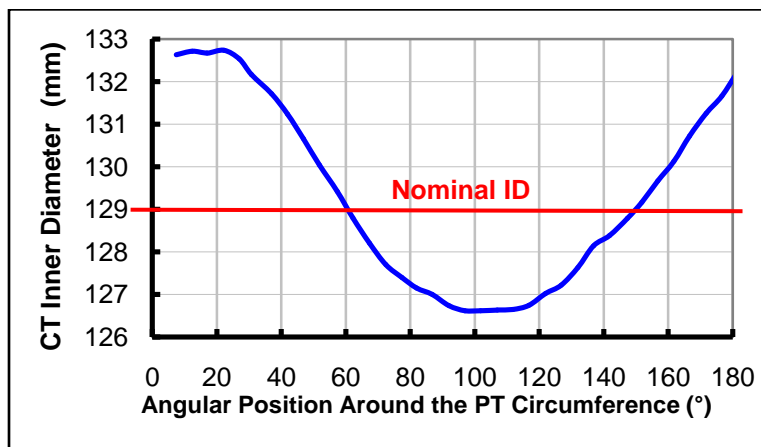


Figure 10. Circumferential CT ID Profile for PLF06 at 4700 mm from the East CTS

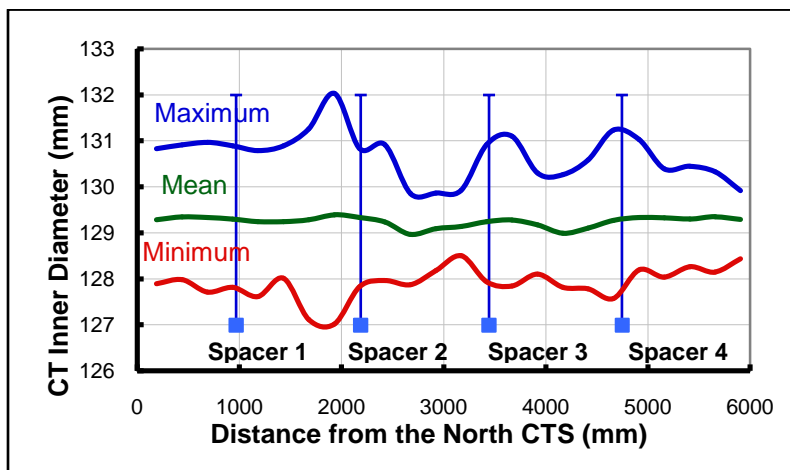


Figure 11. Axial CT ID Profiles for G2H14

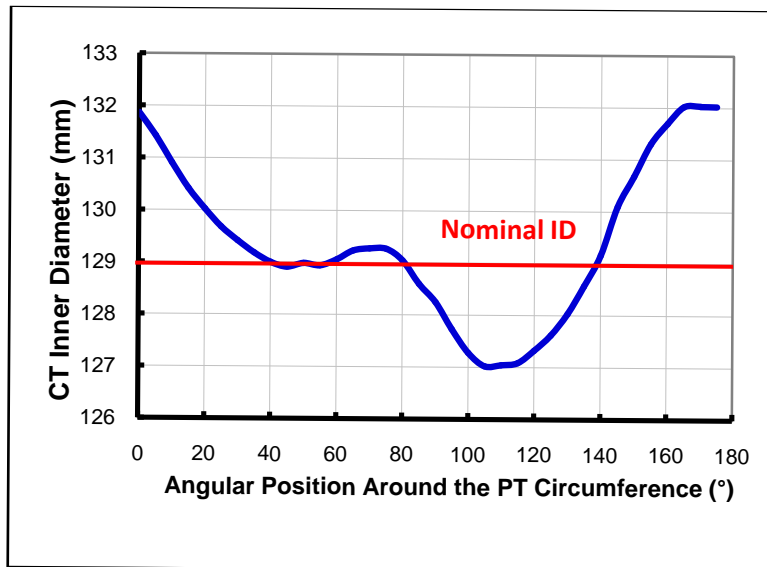


Figure 12. Circumferential CT ID Profile for G2H14 at 1930 mm from the North CTS

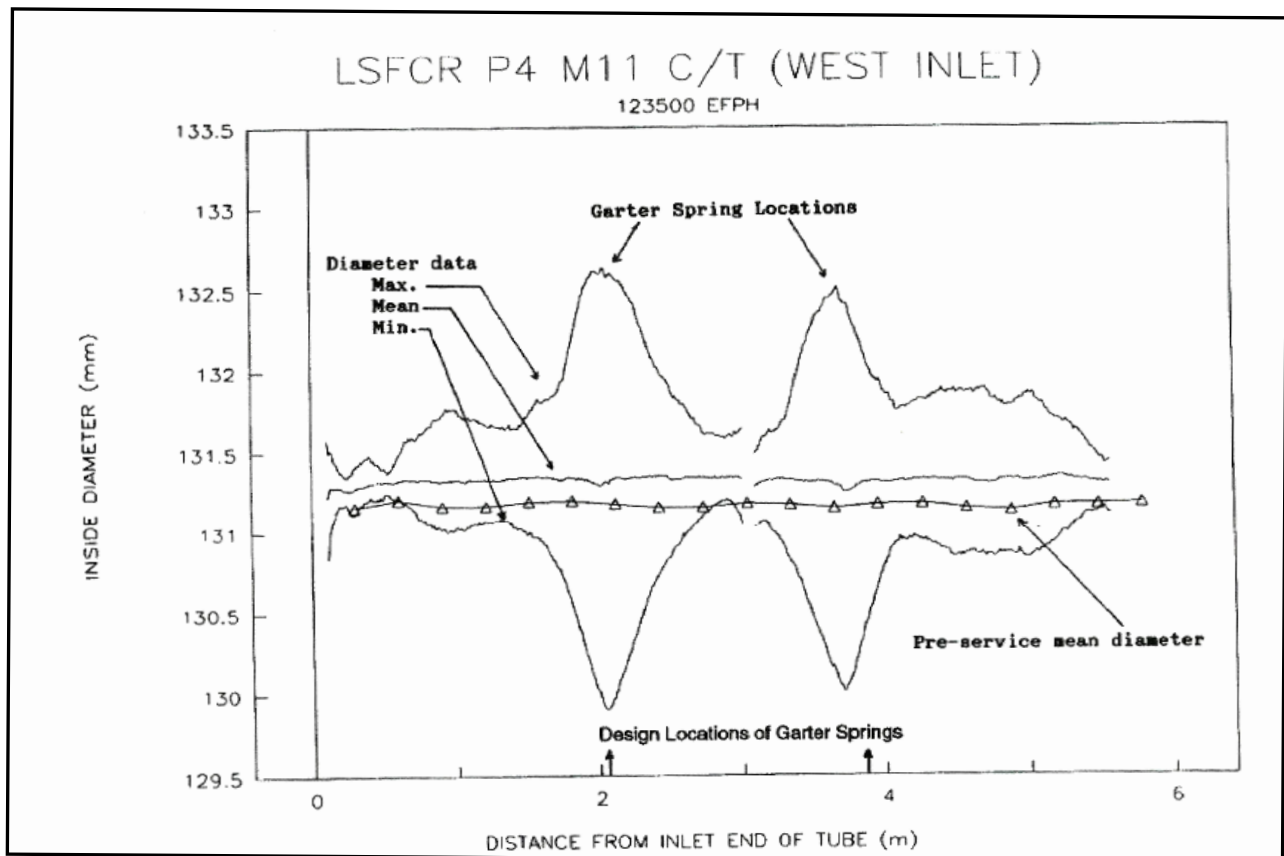


Figure 13. CT Gauging Measurements for P4M11 [2]

## 5.0 Discussion of Results

Figure 13, reproduced from Reference [2], presents axial ID profiles obtained from the post-removal gauging of the CT from P4M11 (Pickering Unit 4). The main features of the CT ID profiles of Figure 13 are deformation peaks that are centred at spacer locations, with uniform average ID values, close to pre-service values, which can serve as benchmarks for a comparison with other CT ID Profiles. Comparing Figures 9 and 11 with Figure 13, it can be seen that the CT ID profiles for PLF06 and G2H14 are similar to that in Figure 13. All three sets of profiles feature local ID maxima and minima at spacer locations, attributable to the local creep deformation of the CT under spacer loading. Noteworthy in Figure 9 are significant variations in the CT average ID above the nominal design value, not present in Figures 11 and 13. It is proposed that the gap calibration scheme used to produce the CT ID profiles of Figure 9 resulted in an overestimation of various gap values, manifested in Figure 9 as an overestimate of the CT average diameter at different points along the CT.

Figures 10 and 12 depict the deformed shape of the CT cross-section at a spacer location, which features increased vertical and decreased horizontal inner diameters, relative to the nominal inner diameter. As an example, in PLF06, the CT vertical diameter has increased by 3.7 mm while the horizontal diameter has decreased by 2.3 mm. Of various possible implications of this deformation, one consideration is the possibility that an ovalised CT could interfere with a spacer during spacer repositioning by contacting the spacer at the 90 and 270 degree locations.

In Figure 10, the CT ID circumferential distribution is quite smooth around the circumference of the CT, as expected. However, in Figure 12, there is an irregularity in the shape of the CT ID profile, of unknown origin, which did not appear in the PLF06 CT ID profiles. Although it is expected that the deformed shape of the CT in G2H14 should be more regular, it is conceivable that some local distortions of the CT shape could occur because of the effects of as-installed residual stresses in the CT, which should be investigated.

## 6.0 Conclusions

1. The un-calibrated gap data examined generally agree reasonably well with expected gap values and the gap measurement profiles have shapes that are reasonable. However, there are consistent, noticeable irregularities in the shape of the circumferential gap profiles where the PT and spacer are in contact.
2. At specific axial locations, some perturbations in the circumferential gap profile shape, of unknown origin, were detected.
3. The calibration of gap measurements, based on spacer outer coil diameter, implies greater CT diametral expansion than that observed in CT gauging measurements [2], indicating that gap calibration may not be technically justifiable.
4. Using G2H14 and PLF06 as examples, reasonable CT ID profiles can be generated using PT inspection data and un-calibrated CT-PT gap data.
5. A significant feature in the CT ID profiles generated for this paper is the development of ovality of the CT cross-section at spacer locations, consisting of an expansion of the vertical axis, and a contraction of

the horizontal axis of the CT. The latter may have implications for spacer movement during spacer repositioning in some channels.

## **7.0 Recommendations**

1. The observed irregularity in the CT ID profile shape of Figure 12 should be investigated, starting with the hypothesis that as-installed CT residual stresses are responsible for distortion of the shape of the CT cross-section.
2. The apparent underestimation of the gap at spacer locations should be investigated to establish whether or not gap calibration can be justified.
3. Once these issues are resolved, it is recommended that CT ID profiles be generated for all inspected FCs so as to develop a database of CT gauging measurements in support of a model for local CT deformation at the spacers.

## **8.0 References**

- [1] Sedran, P.J., Rankin, B., “The Use of OPEX (In the Form of Inspection Data) to Obtain Unanticipated Calandria Tube (CT) Ovality Measurements, 9<sup>th</sup> International Conference on CANDU Maintenance, Toronto, Dec 4 – 6, 2011.
- [2] Song, C., “Evaluation of Calandria Tube Ovality from CANDU Fuel Channel Gauging Data, COG-10-1048, June, 2011.

## **9.0 Acknowledgement**

Dr. Thomas W. Krause was consulted on the topics of circle and point fitting of gap data and contributed to Section 2.1.1 of this paper.